Acta Astronautica 225 (2024) 436–443

Contents lists available at ScienceDirect

Acta Astronautica

journal homepage: www.elsevier.com/locate/actaastro

On the observed time evolution of cosmic rays in a new time domain

C.A. Varotsos [a,b,*], G.S. Golitsyn [c], Y. Mazei [a,d], N.V. Sarlis [e], Y. Xue [f], H. Mavromichalaki [g], M.N. Efstathiou [b]

[a] Faculty of Biology, Shenzhen MSU-BIT University, Shenzhen, 518172, China
[b] Climate Research Group, Division of Environmental Physics and Meteorology, Faculty of Physics, National and Kapodistrian University of Athens, Zografos, 15784, Athens, Greece
[c] Obukhov Institute of Atmospheric Physics, Russian Academy of Sciences, Moscow, Russia
[d] Department of General Ecology and Hydrobiology, Lomonosov Moscow State University, Leninskiye Gory, 1, Moscow, 119991, Russia
[e] Section of Condensed Matter Physics, Department of Physics, National and Kapodistrian University of Athens, Zografos, Greece
[f] School of Emergency Management, Nanjing University of Information Science & Technology, Nanjing, China
[g] Nuclear and particle Physics Department, Faculty of Physics, National and Kapodistrian University of Athens, Zografos, 15784, Athens, Greece

ARTICLE INFO

Keywords:
Cosmic rays
Natural time analysis
Power law
Entropy

ABSTRACT

Since the 1990's, it has been recognized that the full explanation of cosmic rays (CR) and their spectrum may require some new physics. The debate on the origin of CR has led to the conclusion that while most CR come from supernova explosions in the Galaxy, CR with very high energies are likely of extragalactic origin. However, a response to several open questions, still unanswered, concerning CR above 10^{13} eV is required. We herewith study the temporal evolution of the observational CR using data collected by several stations of the ground-based network. The obtained result states that the power spectral density of the CR temporal evolution, especially with a frequency less than 0.1 Hz, exhibits the Kolmogorov-Obukhov 5/3 law that exhibits the energy spectrum of many geophysical quantities. Any small difference found from the 5/3 exponent can be attributed to intermittency corrections and the stations' characteristics. Moreover, natural time analysis applied to the CR time series showed the critical role of the quasi-biennial oscillation to the entropy maximization which occurs following the 5/3 Kolmogorov-Obukhov power law. These findings can be used to more reliably predict extreme CR events that could have an impact even at the molecular level.

1. Introduction

1.1. Cosmic rays nature and impacts

We study cosmic rays (CR), which are the most abundant particles in the universe, and continuously strike Earth's upper atmosphere from outer space. When these energetic particles with energies E > 1 GeV nucleon^{-1} interact with our atmosphere, they produce cascades of secondary particles that fall onto our planet. Their origin includes black holes, supernovae, gamma-ray bursts, and active galactic nuclei. Nowadays, it is believed that the structural preference for chirality in biological molecules may be attributed to the interaction between ancient proto-organisms and CR [1,2].

Cosmic rays are currently studied as they provide insights into extreme phenomena with incredibly high energies. In this regard, the recent discovery of the ultra-high-energy cosmic ray named Amaterasu originating from the Local Void challenges current scientific understanding of CR sources and acceleration mechanisms due to its unprecedented energy levels (exceeding 240 exa-electron volts-EeV). In addition, The Oh-My-God particle, discovered in 1991, holds the record for the highest-energy CR ever detected energy (320 EeV), surpassing the Amaterasu particle. These ultra-high-energy CR are believed to originate from violent astronomical events, like supermassive black holes [3].

According to the International Atomic Energy Agency (IAEA), the average annual radiation exposure for individuals on the ground is approximately 3.5 mSv. Around half of this exposure comes from artificial sources, while the other half is attributed to natural sources, with cosmic radiation accounting for about 10 % of the total. It is important to note that the public dose limit is set at 1 mSv, which carries a 5.5 %

* Corresponding author. Climate Research Group, Division of Environmental Physics and Meteorology, Faculty of Physics, National and Kapodistrian University of Athens, Zografos, 15784, Athens, Greece.
E-mail address: covar@phys.uoa.gr (C.A. Varotsos).

https://doi.org/10.1016/j.actaastro.2024.09.034
Received 22 June 2024; Received in revised form 26 July 2024; Accepted 13 September 2024
Available online 18 September 2024

chance of developing radiation-induced cancer later in life [4].

The assessment of radiation dose from atmospheric neutrons (with energy from 1 to 10^3 MeV) in human tissues reveals a significant increase in these neutrons at higher altitudes and latitudes. For instance, at an elevation of 4 km on a high mountain, the dose is roughly 19 times higher, while at a commercial flight altitude of 10 km, it is about 156 times higher [5].

In the aviation sector, the International Commission on Radiological Protection (ICRP) has suggested reference levels for safeguarding against cosmic radiation to fall within the 5–10 mSv/year range [6]. If the cosmic radiation dose surpasses this reference value, it is classified as an extreme cosmic radiation occurrence. To compute the equivalent dose (Sv), the absorbed dose (Gy) is multiplied by a radiation weighting factor (WR) that is specific to the type of radiation. This factor considers that certain types of radiation present a greater risk to biological tissue, even if their energy deposition levels are identical. For x-rays, gamma rays, and electrons absorbed by human tissue, the WR is 1, while it is 2 for protons and charged pions, (Table 33.1 of [7]). However, for alpha particles, the WR is 20 ([8]; Vajuhudeen, 2024).

Fig. 1 illustrates the CR spectra, or in other words, the CR flux versus energy derived from various experimental campaigns. The point in the CR spectrum where the energy of CR transitions from a power-law to a steeper decline is known as the "knee."

It is believed that the “knee” is caused by either the reduced ability of the galactic magnetic field to confine CR particles with energies above the knee within the galaxy, or it corresponds to the maximum energy that protons can attain through diffusive shock acceleration in supernova remnants.

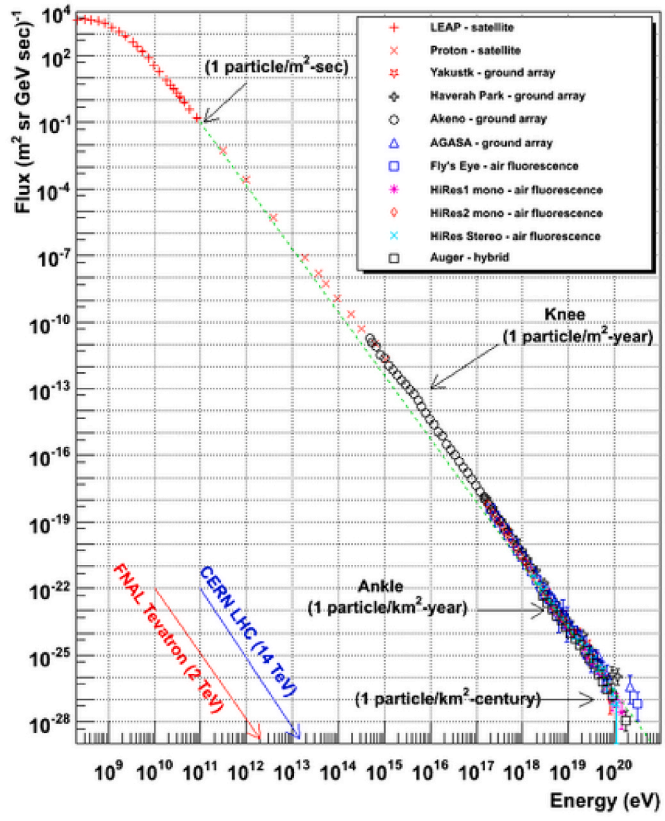

Fig. 1. Cosmic Ray (CR) flux versus particle energy at the top of Earth’s atmosphere. The two features in the CR spectrum, the “knee” and the “ankle” are shown with arrows. This spectrum can be divided into different energy ranges, each with its unique characteristics and distribution of neutron energies. The spectrum ranges from thermal and superthermal neutrons (E < 1eV) with a Maxwellian distribution, to 1eV < E < 50 keV distributed with $E^{3/2}$, to 50 keV < E < 1 MeV depending on slowing down and neutron evaporation processes, and to 1 MeV < E < 10 GeV for fast and relativistic neutrons described by a power function in the higher energy range.

Remarkably, the energies of the spectral "knees" for different CR species are predicted to be proportional to their mass rather than their charge. The “knee” occurs at an energy level that is 2–4 million times greater than the rest mass of the particles. More precisely it is evident from Fig. 1 that when energy levels go up by 10 % past 10^9 eV, the CR amount per area decreases by 10^3 times. But upon closer examination of the spectrum, we notice a “knee” around 10^{15} eV and an “ankle” around 10^{18} eV. The term "ankle" indicates a new CR component, originating from beyond our Milky Way, with cosmic permits from distant galaxies [9].

The power-law energy spectrum of the high-energy CR extends beyond 10^{20}eV, indicating a non-thermal origin. They reveal the relativistic nature of the Universe and shed light on physical processes that surpass what can be achieved in man-made laboratories. It is widely believed that supernovae serve as the primary source of energy for CRs, which diffuse through the interstellar medium and generate secondary particles [10].

The theoretical understanding of the CR spectrum has been anticipated for more than fifty years, with uncertainties surrounding the acceleration of CRs to ultra-relativistic energies of 10^{12} GeV.

A comprehensive comprehension of CRs may require new physics, as Enrico Fermi proposed in 1949 that acceleration could occur at irregularities in the galactic magnetic field [11]. It wasn’t until 2001 that Malkov and Diamond [12] explained that acceleration takes place at collisionless shock wave fronts, and in 2014, the PAMELA experiment revealed a power-law spectrum with an exponent of 2.67. Data from terrestrial measurements also demonstrated a spectrum with an exponent of 2.7 or in cumulative form with an exponent close to 1.7(≈5/3) [13].

CRs play a vital role in comprehending various phenomena, such as Earth’s climate dynamics [14]. Research has indicated that periods of increased solar activity and decreased CR flux are often linked to warmer climates, and vice versa [15]. For instance, Osprey et al. [16] studied muons generated from CR at the Main Injector Neutrino Oscillation Search (MINOS) underground detector revealing sporadic and abrupt spikes in muon levels in the winter season. Muons are a byproduct of CR colliding with the Earth’s atmosphere. When primary CR interact with the atmosphere, the production of charged pions occurs that rapidly decay, resulting in the creation of muons. These muons have weak interactions with matter, allowing them to travel through the atmosphere and even penetrate below the Earth’s surface. Osprey et al. [16] successfully linked these muon spikes to sudden stratospheric warmings (SSWs). In a traditional sense, an SSW indicates a significant increase in stratospheric temperature, sometimes rising by up to 70 °C, lasting for a few weeks in the middle of winter [17].

The motivation of the present paper is the current questions of interest that revolve around various features in the CR energy spectrum. These questions include inquiries about the composition in the knee region and its connection with direct measurements at lower energy levels, the cause of the spectrum’s hardening around 20 PeV, the transition from Galactic to extra-galactic CR and its relation to composition around the ankle, the reason for the apparent end of the spectrum around 100 EeV [18]. More specifically the paper aims to study the temporal evolution of the CR power spectral density using long-term terrestrial observational data and a novel analysis technique.

1.2. *The 5/3 law and its accuracy*

A.N. Kolmogorov [19] outlined numerous probabilistic phenomena in the macrocosm, which are still regarded as empirical laws. These include the Gutenberg – Richter law, elucidating the frequency size distribution, and the turbulence laws ([20], Obukhov 1958, [13,21]). Nevertheless, several other empirical statistical laws in geophysical science remained undiscovered in the mid-20th century.

In 1941, Kolmogorov delved into the statistical properties of turbulence, specifically focusing on the behavior of small-scale structures [null]. During the same year, Obukhov [22] recognized the scale-invariance of energy flux, aligning with Kolmogorov's depiction in real space. The amalgamation of these two led to the development of the Kolmogorov-Obukhov spectrum, which delineates the scaling behavior of energy fluctuations by asserting that the energy spectrum adheres to a power law with an exponent of 5/3. This '5/3' law is crucial as it characterizes the scaling behavior of energy fluctuations in turbulent systems, depicting the energy transfer between various scales.

The 5/3 law holds significant implications in diverse scientific and engineering fields, such as atmosphere-ocean, and astrophysics-cosmology systems. In the former system, the 5/3 law is employed to investigate the core principles that govern critical issues such as predicting storm intensity, regulating the climate through atmosphere-ocean interactions, and studying the development of ocean waves [23]. New experimental findings highlight that the 5/3 law is mostly accurate, however, it may not hold near the ocean surface. This suggests that ocean waves are significant in influencing atmospheric motion and energy balance [24].

Therefore, it is essential to reevaluate the 5/3 law experimentally about flow near ocean waves. As to the astrophysics-cosmology system, turbulence is prevalent in interstellar gas clouds, accretion disks, and galaxy clusters. Thus, astrophysical simulations heavily rely on turbulence models to explore star formation, galaxy evolution, and cosmic magnetic fields. In these models, the 5/3 law is employed and offers valuable insights into energy transfer within cosmic structures.

Considering the information provided above regarding the reliability of the 5/3 law in the atmosphere-ocean system, it is evident that investigating this law through observations in the astrophysics-cosmology system would greatly contribute to enhancing the precision of the models utilized in this field. Exploring CR observations proves to be a fascinating aspect in this regard and is discussed below.

Within the context of the aforementioned motivation and unanswered queries, the central objective of this study is to study the temporal evolution of the CR power spectral density derived from long-term terrestrial observational data. This investigation will shed light on the validity of the 5/3 law in the CR spectrum. Both the conventional and natural time domains will be examined, with a detailed discussion on the latter presented in the following section.

2. Data analysis and methodology

2.1. Instrumentation and data analysis

Neutron monitors (NMs) are CR detectors that utilize gas-filled proportional counters surrounded by various components to detect and measure the flux of secondary CR neutrons, which are slowed down to thermal energies before being detected.

The ground based NMs are the leading instruments for measuring CR and are crucial for research in space physics, solar-terrestrial relations, and space weather applications, as they can detect CR in an energy range that cannot be measured by space detectors. The worldwide network of about 50 stations currently operates two types of standardized detectors (IGY and NM64). The IGY NM was developed by Simpson in the 1950s [25] to study primary CR intensity during the IGY, while the NM64 designed by Carmichael in 1964 [26] became the standard detector for the Quiet Sun Year (IQSY) of 1964, featuring an enhanced counting rate.

For this study, we used the daily CR data of the real-time neutron monitoring stations at the Athens Neutron Monitor Station (A.NE.MO.S) (http://cosray.phys.uoa.gr), Jungfraujoch (Switzerland), and Oulu (Finland) sites provided by the High-Resolution Neutron Monitor DataBase-NMDB (http://www.nmdb.eu/) [27–32]. These stations were selected based on the length of their data time-series. The characteristics of these stations are listed in Table 1.

The effective vertical cutoff rigidity denotes the minimum rigidity a charged particle requires to reach the middle atmosphere in vertical directions (20 km altitude). Research has shown that it almost remains stable for European CR stations (Smart and Shea, 2009; [33]).

Table 1
The list of the stations used in this study for the period 11/2000-10/2023.

Station (Neutron Monitor)	Coordinates	Altitude (above sea level-asl)	Effective vertical cut-off rigidity (GV)	Organization
Athens NM64 (A.Ne.Mo.S)	37.97° N, 23.78° E	260m	8.53	National and Kapodistrian University of Athens, GR.
Jungfraujoch IGY (JIGY) (NM64)	46.55° N, 7.98° E	3570m	4.5	Physikalisches Institut of the Univ. of Bern, CH. Int Foundation & High-Altitude Research Stations Jungfraujoch Gornergrat (HFSJG), Bern CH.
Oulu NM64 station (OULU)	65.05° N, 25.47° E	15m	0.8	Sodankyla Geophysical Obs. of the University of Oulu, FI.

These averages were computed over the period from 2000 to 2017 and then subtracted from the corresponding CR time series for that specific day. Additionally, the long-term trend of the CR time series was eliminated through a 6th-degree polynomial regression analysis.

In the data mentioned above, we utilized a technique called "Natural time analysis" (NTA) introduced in 2001, see Refs. [34,35]). NTA is based on the concept of "Natural time" and disregards the conventional clock time of an event occurrence. Instead, it assigns an index to each event, representing its order of occurrence divided by the total number of events. Further details about NTA are given in the following subsection.

2.2. Methodology: natural time analysis of CR values

With the technique illustrated in Fig. 2 we create a new time series

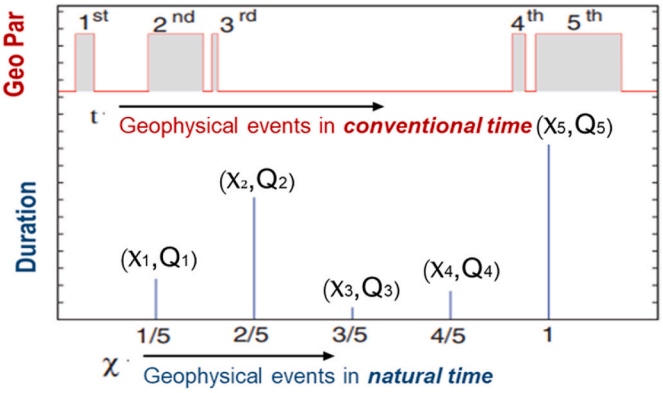

Fig. 2. The time series of signals - events of a geophysical parameter (Geo Par) and the duration of each signal. The "natural time" is a new domain that substitutes the conventional clock time. Specifically, in a time series comprising N events, the "natural time" χ_k is defined as the ratio of the order of appearance k of an event divided by the total number N of events, i.e., $\chi_k = k/N$. Thus, "natural time" displays an index for the occurrence of the k-th event, forgetting the temporal evolution in the conventional clock-time domain. In "natural time" analysis the evolution of the pair of two quantities (χ_k, Q_k) is studied, where Q_k denotes, in general, a quantity proportional to the energy of the individual (k-th) event (i.e., its amplitude or its duration) [34,36,37].

$E_i = (X_i + |X_{min}|)$ with $i = 1, 2, \ldots, N$, where X_i (X_{min}) is the *i-th* event (minimum value) of the original CR dataset and N is the total number of CR events, over the entire period (11/2000-10/2023).

We then use the "natural time" technique, matching each event E_j with the quantity N_j denoting the order of occurrence of E_j against the total number of events within a window of k events, i.e.,

$$\chi_i = N_j = \frac{j}{k}, j = 1, 2, \ldots, k.$$

Thus, we introduce a new sequence of pairs $(\chi_i, Q_j) = (N_j, E_j)$, where Q_j or E_j, is positive and denotes the amplitude or the duration of the signal respectively (Fig. 2). Thus, we use the order of events as a measure of time instead of the conventional clock time (t).

However, the quantity $P_j = \frac{E_j}{\sum_{j=1}^{k} E_j}, j = 1, 2, \ldots, k$, could be considered as a probability, since $P_j > 0$ and $\sum_{j=1}^{k} P_j = 1$, so we try to calculate the entropy of CR events in the natural time domain as follows [34]:

$$S_k = \sum_{j=1}^{k} P_j N_j \, ln(N_j) - \left(\sum_{j=1}^{k} P_j N_j \right) ln\left(\sum_{i=1}^{k} P_i N_i \right) \quad (1)$$

The entropy S_k is calculated for a sliding window of k-length, each time by 1 day, running the entire CR time series of the N-events. Then, we consider the window size $k = 730$ days (2-years) and we calculate S_{730} for the past 730 days and this window is sliding, each time by 1 day, and ran the entire CR time series of N-events. The justification of the choice of this window size is given in section 3.2.

If we consider the effect of the time-reversal in the time series of Q_k the obtained entropy (S'_k) is different from S_k and the quantity $\Delta S_k = S_k - S'_k$ indicates the time symmetry breaking, see, e.g., Sections 7.1 and Appendix A.3 of Varotsos et al. [35]. The approach of the system to a critical point (extreme event) is denoted in advance by a critical value of ΔS_k.

Positive values of ΔS_k correspond to a decreasing time series in natural time and when ΔS_k exceeds a certain threshold, extremely small X_i events (see details in Ref. [35]).

We also calculate the exponent γ of the power law fit to the power spectral density of E_j values ($j = 1, 2, \ldots, k$) as a function of frequency, versus S_k for the above-mentioned sliding window of k-length, running the entire CR time series of the N-events.

3. Results and discussion

3.1. Power spectral density of the CR time-series

We start by investigating the power spectral density of the CR time-series that describes the power present in the CR as a function of frequency, per unit frequency. In Fig. 3 the power-law fit to the profile of the power spectral density for the CR time series in JIGYNM appears to give a better determination than that of the exponential fit. This finding is statistically confirmed, by using F-test, to compare the coefficients of determination for these two distributions, at a 95 % confidence level. Moreover, the Mean Squared Error for both power-law and exponential fit is calculated to measure how close the regression line is to the data points. Remarkably the exponent of the power law is $-1.62(\pm 0.02)$. This exponent confirms the finding of Ginzburg and Syrovatskii [38] that the data for $I(\geq E)$ (i.e., how many particles with energy equal to or greater than E are detected) can be approximated as:

$$I(\geq E) = 1\ E\ (\mathrm{GeV})^{-1.7}\ \text{particles} / \left(\mathrm{cm}^2\ \mathrm{s}\ \mathrm{sr}\right), \text{for } 10\ \mathrm{GeV} < E < 3\mathrm{x}10^6\ \mathrm{GeV}. \quad (2)$$

However, according to Golitsyn [39], the difference in spectral indices 1.62 and 5/3 (as only 1/20) can be ignored in the energy range of 5.5 orders of magnitude.

The same analysis as above was repeated using the CR data collected at JIGYNM but after removing the annual cycle and trend. Then the resulting best fit was obtained with $y = 3.96{\cdot}10^{-6}x^{-1.65}$ and $R^2 = 0.57$, revealing that the exponent of the power law is -1.65 (± 0.02), almost equal to $-5/3$.In the case of OULOU data, the same analysis led to the best-fitting equation $y = 2.14{\cdot}10^{-6}x^{-1.62}$ with $R^2 = 0.61$, where the exponent is $-1.62(\pm 0.02) \approx -5/3$ (see Fig. 4). After deseasonalisation and detrending the best fit is $y = 1.93{\cdot}10^{-6}x^{-1.64}$ with $R^2 = 0.6$.

The Athens station data after the implementation of the same analysis resulted in the following best fit: $y = 3.21{\cdot}10^{-7}x^{-1.56}$ with $R^2 = 0.56$, where the exponent is -1.56 (± 0.02). No significant change is observed when the annual cycle and trend are removed from the CR time series (see Fig. 5). It is noteworthy that there is not any time lag between the data collected in these three observatories. However, the extracted exponent in the Athens data set deviates the most from $-5/3$.

To interpret the above-mentioned results for the power spectral density of CR it is worth recalling the following theoretical approach to the problem [11].

Following Fermi's idea of the acceleration of CR particles at collisionless shock wave fronts, the energy volume density of CR particles is

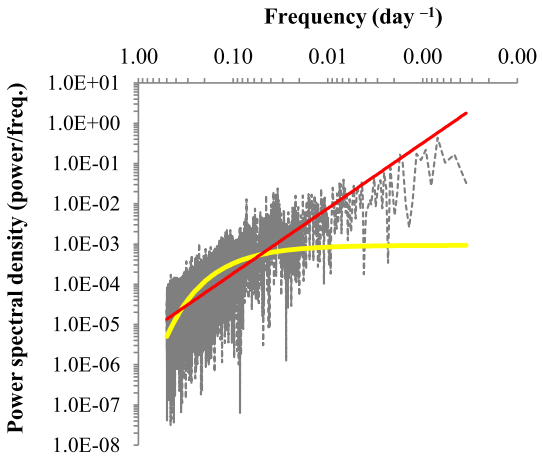

Fig. 3. The power spectral density for the initial CR time series at JIGYNM, with the corresponding power-law (red line) and exponential (yellow line) fit ($y = 4.41{\cdot}10^{-6}x^{-1.62}$, with $R^2 = 0.59$ and $y = 9.28{\cdot}10^{-4}e^{-10.4}x$, with $R^2 = 0.52$). (For interpretation of the references to colour in this figure legend, the reader is referred to the Web version of this article.)

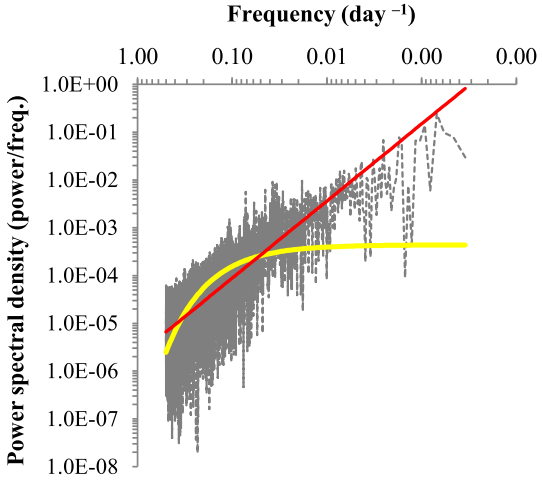

Fig. 4. As in Fig. 3, but at OULOU, with the corresponding power-law (red line) and the exponential (yellow line) fit ($y = 2.14{\cdot}10^{-6}x^{-1.62}$, with $R^2 = 0.61$ and $y = 4.38{\cdot}10^{-4}e^{-10.4}x$, with $R^2 = 0.54$). (For interpretation of the references to colour in this figure legend, the reader is referred to the Web version of this article.)

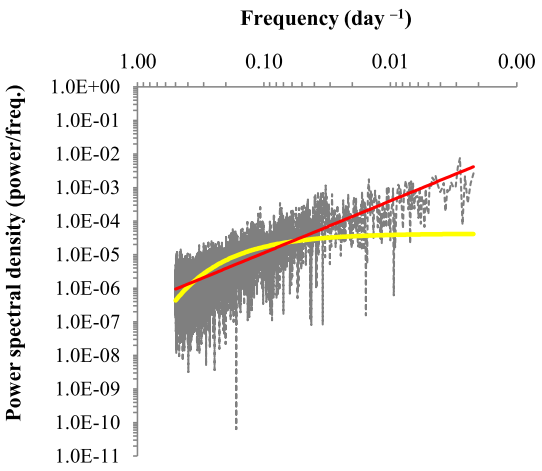

Fig. 5. As in Fig. 3, but in Athens, with the corresponding power-law (red line) and exponential (yellow line) fit ($y = 3.21{\cdot}10^{-7}x^{-1.56}$, with $R^2 = 0.56$ and $y = 4.26{\cdot}10^{-5}e^{-9.2}x$, with $R^2 = 0.46$). (For interpretation of the references to colour in this figure legend, the reader is referred to the Web version of this article.)

around $w_o \approx 0.5$ eV/cm$^3 \approx 10^{-13}$ J/m^3 [40].

It should be emphasized that assuming a mean galactic field intensity of 5×10^{-6} Oe, we find $H^2/8\pi \approx 10^{-13}$ J/m^3. This observation was made by Ginzburg and Syrovatskii [38], who proposed that this equality is a result of the interactions between CR and the magnetic field. If the energy of the magnetic field were higher, it would be able to confine a greater number of continuously generated particles. Conversely, if the energy were lower, the excess particles would quickly escape from the galaxy.

The counted particles' number per unit of time, area, and angle with energies $E \pm dE$ provides the energy spectrum. The integral spectrum dimensions $[I(\geq E)] = L^{-2}T^{-1}$ the CR energy volume density $[w_o] = EL^{-3/2}$, the production rate G, $[G] = ET^{-1}$ and the energy itself $[E] = E$ is used.

Then $I(\geq E) = G^{-1}\, w_o^{-k} E^l$ and $i =$

$$-1, k = 2 \;\Big/\; 3, l = -5 \;\Big/\; 3, \text{or } I(\geq E) = a_1 \frac{G}{E}\left(\frac{w_0}{E}\right)^{2/3} \sim E^{-5/3}, \qquad (3)$$

where $\alpha_1 \sim 10^{-27}$ [41].

When we compare the exponent $-5/3$ of relation (3) with the exponent -1.56 obtained for Athens, we notice that they differ by just 1/30 approximately. This slight difference can be ignored across the energy span of 5.5 orders of magnitude; the highest deviation will not surpass 40 % [41].

The power-law fitting exponents shown in Figs. 3–5 are derived by applying regression analysis and their statistical significance is certified at 95 % confidence level using a *t*-test. Therefore, the main conclusion drawn from our analysis is that the power spectral density exponent of the CR measurements made by the ground-based network over several decades confirms the theoretically derived value of around $-5/3$, for frequencies lower than 10^{-1} Hz. However, it should be emphasized that the basic problem is not to obtain Kolmogorov–Obukhov indicator $-5/3$ only, but rather to obtain a value for μ, where the exponent should be $-5/3 + \mu$, due to intermittency corrections.

This observation aligns with the evidence that research on cosmic ray fluxes, specifically examining the "knee" (slightly below 10^{16} eV) and the "ankle" (around 10^{19} eV), encompasses phenomena like turbulence [42]. Related to this, determining the CR particles source and the formation mechanism of the observed "knee" and "ankle" in the CR differential energy spectrum obeying a power law near $-8/3$, is still an unsolved problem [43].

3.2. On the relationship between entropy and the power-law exponent of CR temporal evolution

In the following, we apply the natural time analysis described briefly in subsection 2.2. Using Eq. (1)the entropy S_k is calculated for a sliding window of k-length, each time by 1 day, running the entire CR time series of the N-events. Then, we consider the window size $k = 730$ days (2-years) and we calculate S_{730} for the past 730 days and this window is sliding, each time by 1 day, and ran the entire CR time series of N-events.

The selection of the 2-year window size was not arbitrary. The equatorial lower and middle stratosphere goes through a regular cycle known as the quasi-biennial oscillation (QBO). This cycle lasts for 2–3 years (average period 28 months) and is characterized by alternating patterns of westward and eastward zonal wind. Along with the zonal wind, the QBO also brings changes in temperature, trace constituents, and mean meridional circulation. The QBO has a significant impact on the equatorial lower and middle stratosphere and affects other parts of the atmosphere, such as the tropical troposphere, tropical upper stratosphere and mesosphere, the extratropical middle atmosphere during winter, and sudden stratospheric warmings of the high latitudes [44]. Thus, the QBO influences climate phenomena beyond the tropical stratosphere, including O_3 transport, the North Atlantic, and the Madden-Julian Oscillations [45]. However, simulating the QBO is challenging due to uncertainties surrounding the waves that drive the oscillation, particularly the momentum fluxes from small-scale gravity waves caused by deep convection.

Despite the complexity and unpredictability of these wave motions, the predictability of the QBO is remarkable, considering their wide range of spatial and temporal scales. Hopefully, by improving our understanding of the processes that control the QBO, we can also gain insight into unexpected events like the two QBO disruptions observed since 2016. Varotsos et al. [46] investigated the unusual equatorial QBO event in the zonal wind in 2016 and suggested that it was not related to any previous events. They used NTA to analyze the QBO data and found a precursor behavior before the increase in zonal wind velocity, indicating a possible connection with the strong El Niño event in 2015–2016. In addition, our previous research on the dynamics of the ozone hole in the Antarctic and the El Niño phenomenon showed that a window of approximately 2–3 years was optimal for detecting critical system states [47–53]

Since the CR data utilized in this study were collected from instruments on the ground, it is logical to consider that they may be influenced by natural atmospheric fluctuations, like the QBO [54]. This is why we opted for a 2-year window size as the threshold for our NTA analysis.

Consequently, considering the potential impact of QBO on the CR flux reaching the ground, we calculated the exponent γ of the power-law fit to the power spectral density of Ej values (j = 1,2, .., k) as a function of frequency, compared to S_k using the sliding window of length k. This analysis was performed on the entire CR time series of the N-events at OULU station.

Bearing in mind the afore-mentioned discussion on the potential influence of the QBO to the CR flux reaching the ground, we proceed to calculate the exponent γ of the power-law fit to the power spectral density of E_j values ($j = 1, 2, \ldots, k$) as a function of frequency, versus S_k employing the above-mentioned sliding window of k-length, running the entire CR time series of the N-events at OULU station.

The results obtained are shown in Fig. 6 where plots of the γ-exponent versus S_{730} for the CR dataset at OULU station smoothed by applying the 30-day running mean (red line) are presented. It can be seen that the γ-value varies from -1.9 to -1.3, as the sliding window of 730-length runs the entire CR time series. Moreover, it is noteworthy from Fig. 6 that the maximum value of S_{730} is observed for $\gamma = -1.67 = -5/3$.

It should be emphasized that for the uniform distribution (u), (e.g. when our system is in a stationary state emitting uncorrelated bursts of

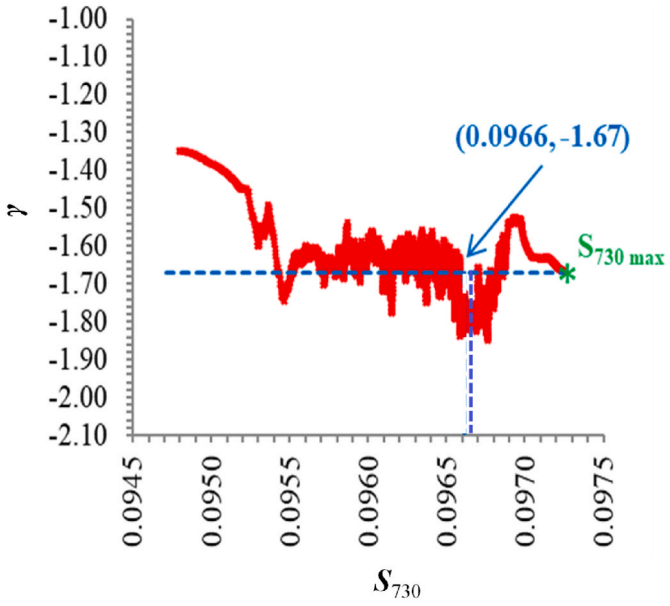

Fig. 6. Power law exponent γ of the E_j values ($j = 1,2,\ldots,730$) as a function of frequency versus S_{730}, for the above-mentioned sliding window of 730-length, running the entire CR time series of the N-events at OULU station, expressed as 30-day running mean of the data (red line). Interestingly, we find that one of the points with S_{730}=S_u (=0.0966) corresponds to $\gamma = -5/3 \approx -1.67$ (blue coordinates and green star). (For interpretation of the references to colour in this figure legend, the reader is referred to the Web version of this article.)

energy) Eq. (1) gives the entropy S_u of the uniform distribution [34]:

$$S_u = (\ln 2)/2 - 1/4 \approx 0.0966,$$

where $\gamma = -1.67$ (see Fig. 6).

This is reminiscent of the fact that according to Varotsos et al. [55] the experimental data of systems emitting energy bursts, when analyzed by NTA, show that they obey a power-law distribution with an exponent γ between 1.5 and 2.1. For example, this exponent is between 1.5 and 2.1 in solar flares, and 1.5–1.8 in earthquakes and takes the value 1.8 in the case of icequakes. Consequently, this very important result may be used for the prediction modelling of the CR extreme events and their interplay with other geophysical phenomena.

Next, the same analysis was conducted on the data collected at JIGYNM and Athens stations (see Fig. 7). The results indicate that the power law exponent corresponding to the maximum S_{730} value is $\gamma = -1.59$ and $\gamma = -1.54$ at JIGYNM and Athens stations, respectively. Both values deviate from the -1.67 ($-5/3$) that was found at OULOU. It is noticeable that the exponent's value displays the most significant deviation from $-5/3$ in the data from Athens' station, the southernmost station. This variation could be attributed to the notably higher maximum effective vertical cut-off rigidity at the Athens station, which exceeds that of OULU by more than tenfold. It is essential to emphasize that magnetic rigidity is defined as the momentum of a charged particle divided by its electric charge, then multiplied by the speed of light.

This fundamental quantity plays a critical role in studying the motion of charged particles within a magnetic field, as particles with the same rigidity and initial conditions will follow identical paths in a specific magnetic field. This does not hold in the case of the selected three stations, in our study.

It should be stressed that variations in atmospheric parameters impact the generation multiplicity of CR secondary particles, with barometric and temperature effects playing a significant role. While the neutron component is mainly influenced by barometric effects (taken into account in the data used here), there is evidence of a humidity effect that has been historically overlooked but may have an impact on CR neutron intensity near Earth's surface [56–58].

Neutrons formed in the atmosphere through interactions with CR undergo elastic collisions, losing energy and eventually being absorbed. The rate of neutron production in the atmosphere remains constant, but variations in water vapor content cause intensity variations in the detected neutron component [59]. Furthermore, the neutron flux density near Earth's surface is inversely proportional to air and soil humidity [60]. Although the humidity effect is much less than the barometric one, the neutron energy spectrum displays information about moisture.

As highlighted in the Introduction, CR flux is connected to climate change. Hence, climate modeling must incorporate our findings for enhancement. For instance, CRs ionize the atmosphere, forming cloud condensation nuclei leading to cloud formation acting like an "umbrella". For example, when the CR flux decreased (because of the increased solar wind from sunspots), there was a decrease in cloud cover, which could potentially lead to warming (Svensmark et al., 2007,

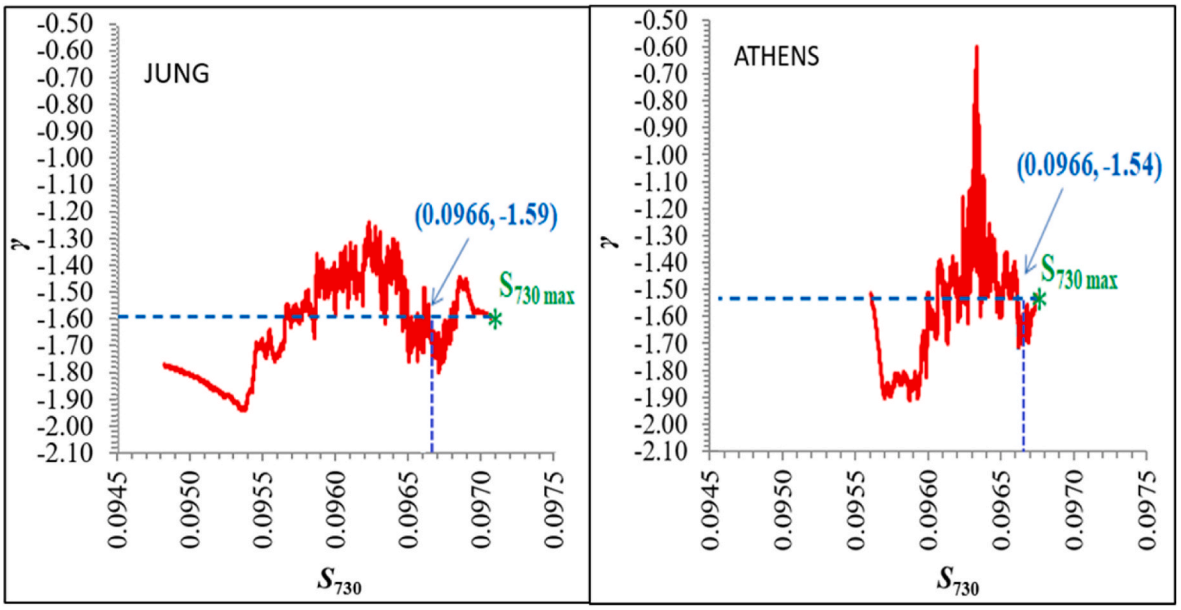

Fig. 7. As in Fig. 6, but for the stations JUNG and Athens.

[61]). Some scientists, however, have raised doubts about the connection between CR and cloud cover and argue that just because there is a correlation doesn't mean there is causation [62].

4. Conclusions

From the above analysis and discussion, it follows that the observed temporal evolution of CR deduced from several stations of the terrestrial network exhibits a power spectral density consistent with the finding that the energy spectrum of CR obeys the Kolmogorov-Obukhov 5/3 law, which has already been confirmed in several geophysical quantities [41,55].

It is observed even more so when the frequency is less than 10^{-1} day^{-1}. Furthermore, with the natural time analysis, we showed that the 5/3 Kolmogorov-Obukhov power law is also related to the maximum value of CR entropy in which the QBO was revealed as a leading index. This CR behaviour is consistent with the finding that systems emitting energy bursts (such as solar flares, earthquakes, and icequakes) obey a power-law distribution with an exponent between 1.5 and 2.1.

This may be used for the prediction of the CR extreme events, as in prediction problems maximized entropy gives the maximum room for the data to reveal secrets hidden and ensures that no unconscious arbitrary assumptions are introduced into the method used [63,64].

As mentioned in the introduction there are several unanswered questions in the CR domain, such as the origin and mass composition of ultra-high energy CR and how they achieve extreme energies [65]. These questions drive ongoing research and exploration, pushing the boundaries of our understanding of CR and the universe. Geophysical research is gaining significance as we enter a period of rapidly increasing natural disasters in the upcoming decades. It is increasingly imperative considering that CR have made a lasting mark on early life and could have affected certain crucial biological aspects with potential consequences.

Funding

This research received no external funding.

CRediT authorship contribution statement

C.A. Varotsos: Writing – original draft, Supervision, Investigation, Conceptualization. **G.S. Golitsyn:** Validation, Methodology, Formal analysis. **Y. Mazei:** Validation, Resources, Methodology. **N.V. Sarlis:** Methodology, Investigation, Data curation. **Y. Xue:** Visualization, Investigation, Data curation. **H. Mavromichalaki:** Resources, Methodology, Formal analysis, Data curation. **M.N. Efstathiou:** Software, Methodology, Formal analysis, Data curation.

Declaration of competing interest

The authors declare that they have no known competing financial interests or personal relationships that could have appeared to influence the work reported in this paper.

Acknowlwdgments

This work was accomplished as part of the IAA Study (1.16) entitled: Nowcasting Extreme Cosmic Ray Events.We acknowledge the NMDB database www.nmdb.eu, founded under the European Union's FP7 programme (contract no. 213007) for providing data.", and individual monitors following the information given on the respective station information page (www.nmdb.eu).

References

[1] N. Globus, R.D. Blandford, The chiral puzzle of life, Astrophys. J. Lett. 895 (1) (2020) L11, https://doi.org/10.3847/2041-8213/ab8dc6.
[2] T. Kubota, Cosmic rays may have left indelible imprint on early life, Stanford physicist says. Stanford News (2020). https://news.stanford.edu/2020/05/20/cosmic-rays-may-shaped-life/.
[3] Telescope Array Collaboration, et al., An Extremely Energetic Cosmic Ray Observed by a Surface Detector Array, Science382, 2023, pp. 903–907, https://doi.org/10.1126/science.abo5095.
[4] L. Gil, Cosmic radiation: why we should not be worried, IAEA Office of Public Information and Communication (2021). https://www.iaea.org/newscenter/news/cosmic-radiation-why-we-should-not-be-worried.
[5] R. Sparvoli, M. Martucci, Advances in the research on cosmic rays and their impact on human activities, Appl. Sci. 12 (2022) 3459, https://doi.org/10.3390/app12073459.
[6] ICRP, The 2007 recommendations of the international commission on radiological protection, ICRP Publication 103. Ann. ICRP 37 (2–4) (2007).
[7] Beringer, et al., Review of particle physics, Phys. Rev. D 86 (1) (2012) 010001, https://doi.org/10.1103/PhysRevD.86.010001.
[8] J.E. Martin, Physics for Radiation Protection, third ed., Wiley-VCH, 2013. ISBN-13: 978-3527411764.
[9] W.D. Apel, J.C. Arteaga-Velàzquez, K. Bekk, M. Bertaina, J. Blümer, H. Bozdog, I. M. Brancus, E. Cantoni, A. Chiavassa, F. Cossavella, K. Daumiller, Ankle-like feature in the energy spectrum of light elements of cosmic rays observed with KASCADE-Grande, Phys. Rev. D 87 (8) (2013) 081101, https://doi.org/10.1103/PhysRevD.87.081101.
[10] D'Ettorre Piazzoli Benedetto, et al., Chapter 4 cosmic-ray physics, Chin. Phys. C 46 (2022) 030004, https://doi.org/10.1088/1674-1137/ac3faa.
[11] G.S. Golitsyn, AN Kolmogorov's 1934 paper is the basis for explaining the statistics of natural phenomena of the macrocosm, Usp. Fiz. Nauk 194 (1) (2024) 86–96.
[12] M.A. Malkov, P.H. Diamond, Modern theory of Fermi acceleration: a new challenge to plasma physics, Phys. Plasmas 8 (5) (2001) 2401–2406.
[13] G.S. Golitsyn, Probability Structures of the Macroworld: Earthquakes, Hurricanes, Floods, Fizmatlit, 2022.
[14] A.S. Chefranov, S.G. Chefranov, G.S. Golitsyn, Cosmic rays self-arising turbulence with universal Spectrum− 8/3, Astrophys. J. 951 (1) (2023) 38.
[15] I.G. Usoskin, M. Schüssler, S.K. Solanki, K. Mursula, Solar activity, cosmic rays, and Earth's temperature: a millennium-scale comparison, J. Geophys. Res.: Space Phys. 110 (A10) (2005).
[16] S. Osprey, et al., Sudden stratospheric warmings seen in MINOS deep underground muon data, Geophys. Res. Lett. 36 (2009) L05809, https://doi.org/10.1029/2008GL036359.
[17] C.A. Varotsos, A.P. Cracknell, C. Tzanis, Major atmospheric events monitored by deep underground muon data, Remote Sensing Letters 1 (3) (2010) 169–178.
[18] T. Gaisser, Challenges for cosmic-ray experiments, in: EPJ Web of Conferences, vol. 145, EDP Sciences, 2017, p. 18003, https://doi.org/10.1051/epjconf/201714518003.
[19] A.N. Kolmogorov, ZufalligeBewegungen, Ann. Math. 35 (1934) 116–117.
[20] P.W. Bridgman, Dimensional Analysis, 2-nd ed., Yale Univ. Press, 1932, 1921 (1st ed.).
[21] B. Birnir, The Kolmogorov–Obukhov statistical theory of turbulence, J. Nonlinear Sci. 23 (2013) 657–688, https://doi.org/10.1007/s00332-012-9164-z.
[22] A.M. Obukhov, On the distribution of energy in the spectrum of turbulent flow, Dokl. Akad. Nauk SSSR 32 (1941) 19.
[23] D.G. Ortiz-Suslow, Q. Wang, An evaluation of Kolmogorov's −5/3 power law observed within the turbulent airflow above the ocean, Geophys. Res. Lett. 46 (2019) 14901–14911, https://doi.org/10.1029/2019GL085083.
[24] D.G. Ortiz-Suslow, Q. Wang, Direct measurement of the inertial-convective subrange above ocean surface waves, Phys. Fluids 36 (2024) 2, https://doi.org/10.1063/5.0178922.
[25] J.A. Simpson, Cosmic Radiation Neutron Intensity Monitor, Annals of the Int. Geophysical Year, vol. IV, Pergamon Press, London, 1958, p. 351. Part vol. II.
[26] H. Carmichael, IQSY Instruction Manual, vol. 7, Deep River, Canada, 1964.
[27] J. Christodoulakis, C.A. Varotsos, H. Mavromichalaki, M.N. Efstathiou, M. Gerontidou, On the link between atmospheric cloud parameters and cosmic rays, J. Atmos. Sol. Terr. Phys. 189 (2019) 98–106.
[28] H. Mavromichalaki, World-wide Integration of Neutron Monitors-The NMDB Project, EOS AGU, 2010, pp. 305–306, 31.8.2010.
[29] H. Mavromichalaki, et al., Applications and usage of the real – time neutron monitor database, Adv. Space Res. 47 (2011) 2210–2222.
[30] C.A. Varotsos, G.S. Golitsyn, M. Efstathiou, N. Sarlis, A new method of nowcasting extreme cosmic ray events, Remote Sensing Letters 14 (6) (2023) 576–584.
[31] C.A. Varotsos, G.S. Golitsyn, Y. Xue, M. Efstathiou, N. Sarlis, T. Voronova, On the relation between rain, clouds, and cosmic rays, Remote Sensing Letters 14 (3) (2023) 301–312.
[32] I. Xaplanteris, et al., Improved approach in the coupling function between primary and ground level cosmic ray particles based on neutron monitor data, Sol. Phys. 296 (91) (2021), https://doi.org/10.1007/s11207-021-01836-y.
[33] M. Gerontidou, N. Katzourakis, H. Mavromichalaki, V. Yanke, E. Eroshenko, World grid of cosmic ray vertical cut-off rigidity for the last decade, Adv. Space Res. 67 (7) (2021) 2231–2240, https://doi.org/10.1016/j.asr.2021.01.011.
[34] P.A. Varotsos, N.V. Sarlis, E.S. Skordas, M.S. Lazaridou, Entropy in the natural time domain, Phys. Rev. 70 (2004) 011106, https://doi.org/10.1103/PhysRevE.70.011106.

[35] P.A. Varotsos, N.V. Sarlis, E.S. Skordas, Natural Time Analysis: the New View of Time. Part II. Advances in Disaster Predictions Using Complex Systems, Springer-Verlag, Berlin Heidelberg, 2023, https://doi.org/10.1007/978-3-031-26006-3.
[36] P.A. Varotsos, N.V. Sarlis, E.S. Skordas, Order parameter fluctuations in natural time and b-value variation before large earthquakes, Nat. Hazards Earth Syst. Sci. 12 (11) (2012) 3473–3481, https://doi.org/10.5194/nhess-12-3473-2012.
[37] N.V. Sarlis, E.S. Skordas, S.-R.G. Christopoulos, P.A. Varotsos, Natural time analysis: the area under the receiver operating characteristic curve of the order parameter fluctuations minima preceding major earthquakes, Entropy 22 (583) (2020), https://doi.org/10.3390/e22050583.
[38] V.L. Ginzburg, S.I. Syrovatskii, The secondary electron component of cosmic rays and the spectrum of general galactic radio emission, Sov. Astron. 8 (1964) 342.
[39] G.S. Golitsyn, Spectrum of cosmic rays from the point of view of the similarity theory, Astronomy Lett 23 (2) (1997) 149–154.
[40] V.L. Ginzburg (Ed.), Astrophysics of Cosmic Rays, North Holland Publ. Co, Amsterdam, 1990.
[41] G.S. Golitsyn, Random moves equation Kolmogorov-1934. A unified approach for description of statistical phenomena of nature, arXiv preprint arXiv:2310.06057 (2023).
[42] C. Tsallis, J.C. Anjos, E.P. Borges, Fluxes of cosmic rays: a delicately balanced stationary state, Phys. Lett. 310 (5–6) (2003) 372–376.
[43] J.S. Niu, Origin of hardening in spectra of cosmic ray nuclei at a few hundred GeV using AMS-02 data, Chin. Phys. C 45 (4) (2021) 041004.
[44] C. Varotsos, M. Efstathiou, C. Tzanis, Scaling behaviour of the global tropopause, Atmos. Chem. Phys. 9 (2) (2009) 677–683.
[45] J.A. Anstey, S.M. Osprey, J. Alexander, et al., Impacts, processes and projections of the quasi-biennial oscillation, Nat. Rev. Earth Environ. 3 (2022) 588–603, https://doi.org/10.1038/s43017-022-00323-7.
[46] C. Varotsos, N.V. Sarlis, M. Efstathiou, On the association between the recent episode of the quasi-biennial oscillation and the strong El Niño event, Theor. Appl. Climatol. 133 (2018) 569–577, https://doi.org/10.1007/s00704-017-2191-9.
[47] M.N. Efstathiou, C. Tzanis, A.P. Cracknell, C.A. Varotsos, New features of land and sea surface temperature anomalies, Int. J. Rem. Sens. 32 (11) (2011) 3231–3238.
[48] C.A. Varotsos, C. Tzanis, A new tool for the study of the ozone hole dynamics over Antarctica, Atmos. Environ. 47 (2012) 428–434, https://doi.org/10.1016/j.atmosenv.2011.10.038.
[49] C.A. Varotsos, C.G. Tzanis, N.V. Sarlis, On the progress of the 2015–2016 El Niño event, Atmos. Chem. Phys. 16 (4) (2016) 2007–2011.
[50] C. Varotsos, N.V. Sarlis, Y. Mazei, D. Saldaev, M. Efstathiou, A composite tool for forecasting el-nino. The case of the 2023–2024 event, Forecasting 6 (1) (2024) 187–203.
[51] C. Varotsos, Atmospheric pollution and remote sensing: implications for the southern hemisphere ozone hole split in 2002 and the northern mid-latitude ozone trend, Adv. Space Res. 33 (3) (2004) 249–253.
[52] C. Varotsos, Re-evaluation of surface ozone over Athens, Greece, for the period 1901–1940, Atmos. Res. 26 (4) (1991) 303–310.
[53] A.P. Cracknell, The present status of the total ozone depletion over Greece and Scotland: a comparison between Mediterranean and more northerly latitudes, Int. J. Rem. Sens. 16 (10) (1995) 1751–1763.
[54] M.J. Kang, H. Kim, S.W. Son, QBO modulation of MJO teleconnections in the North Pacific: impact of preceding MJO phases, npj Clim Atmos Sci 7 (2024) 12, https://doi.org/10.1038/s41612-024-00565-w.
[55] P. Varotsos, N. Sarlis, E. Skordas, M. Lazaridou, Attempt to distinguish long-range temporal correlations from the statistics of the increments by natural time analysis, Phys. Rev. 74 (12) (2006) 021123, https://doi.org/10.1103/PhysRevE.74.021123.
[56] L.I. Dorman, Variatsii Kosmicheskikh luchey[Variations of Cosmic Rays], Gostechizdat Publ., Moscow, 1957, p. 285 (In Russian).
[57] L.I. Dorman, Meteorologicheskie Effekty Kosmicheskikh Lu-chei[Meteorological Effects of Cosmic Rays], NaukaPubl., Moscow, 1972, p. 211 (In Russian).
[58] L.I. Dorman, Eksperimentalnye I Teoreticheskie Osnovy As-Trofiziki Kosmicheskikh Luchei [Experimental and Theoretical Foundations of Cosmic Ray Astrophysics], Nauka Publ., Moscow, 1975, p. 462 (In Russian).
[59] M. Zreda, W.J. Shuttleworth, X. Zeng, C. Zweck, D. Desilets, T. Franz, R. Rosolem, COSMOS: the COsmic-ray soil moisture observing system, Hydrol. Earth Syst. Sci. 16 (2012) 4079–4099, https://doi.org/10.5194/hess-16-4079-2012.
[60] Yanchukovsky, M.A. Kalyuzhnaya, R.Z. Khisamov, Intensity of the neutron component of cosmic rays and air humidity, Solar-Terrestrial Physics 10 (1) (2024) 34–39, https://doi.org/10.12737/stp-101202405.
[61] H. Svensmark, M.B. Enghoff, N.J. Shaviv, et al., Increased ionization supports growth of aerosols into cloud condensation nuclei, Nat. Commun. 8 (2017) 2199, https://doi.org/10.1038/s41467-017-02082-2.
[62] A. Erlykin, T. Sloan, A. Wolfendale, Cosmic rays and climate, Phys. World 24 (10) (2011) 25.
[63] E.T. Jaynes, Information theory and statistical mechanics, Physical review 106 (4) (1957) 620.
[64] E.T. Jaynes, Probability Theory: the Logic of Science, Cambridge university press, 2003. ISBN 0-521-59271-2.
[65] R. Alves Batista, J. Biteau, M. Bustamante, K. Dolag, R. Engel, K. Fang, M. Unger, Open questions in cosmic-ray research at ultrahigh energies, Frontiers in Astronomy and Space Sciences 6 (2019) 23.